



# AN ANALYTICAL EVALUATION OF THE CO-VARIATIONS AMONG LOCAL MORAN'S $I_i$ IN AUTOCORRELATED MAP PATTERNS

by

***Michael Tiefelsdorf***

tiefelsdorf@utd.edu

The University of Texas at Dallas

***Sweta Jinnagara Puttaswamy***

The University of Texas at Dallas

Paper presented at the North-American Regional Science Association  
Denver, November 10-13, 2010

# INTRODUCTION: LISA

- ✗ Local indicators of spatial association (LISA) are frequently used to identify
  - + **Local misspecifications** of the first order trend component.
  - + **Heterogeneities** within the stochastic second order component of a spatial processes.
- ✗ Communal assessment of a set of LISA's and multiple comparisons requires
  - + knowledge of their **joint distribution**, which has to be
  - + conditional to an underlying global **spatial process**.
- ✗ Knowledge of the pairwise **correlations** among LISAs is a step towards a solution of the multiple comparison problem.

## Focus of this study

- ✗ Results are shown for the **correlation** among **local Moran's  $I_s$**  subject to a global spatial process in **hexagonal** tessellations.
- ✗ Several **cross-checks** were performed, analytical results against simulation results.



# DEVELOPMENTS AROUND MORAN'S $I$

## ✖ Past:

- + *Moran*, 1950. Proposal of the spatial autocorrelation test statistic
- + *Imhof*, 1961. Univariate distribution through numerical inversion
- + *Sawa*, 1978. Higher order conditional moments
- + *Shepard*, 1991. Joint distribution through multivariate numerical inversion.
- + *Anselin*, 1995, Introduction of the local Moran's  $I_i$  concept.  
⇒ Reformulated by *Tiefelsdorf*, 1996, as a ratio of quadratic forms.
- + *Tiefelsdorf*, 1998. Exact conditional distribution
- + *Tiefelsdorf*, 1998. First exploration of conditional **correlation**.

## ✖ Present:

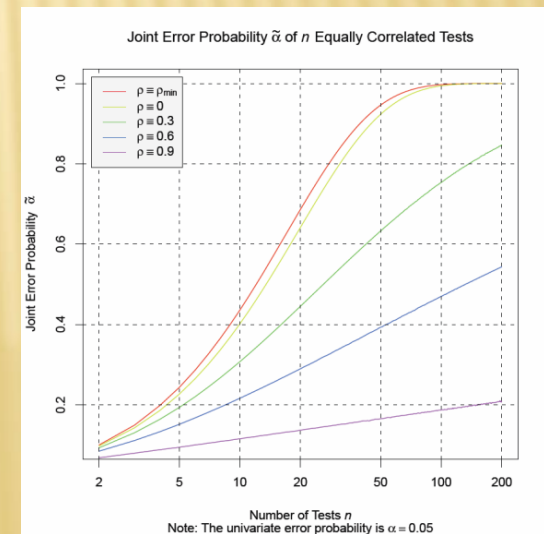
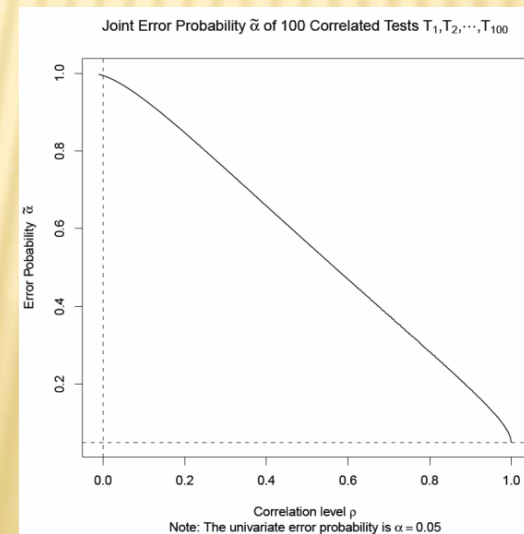
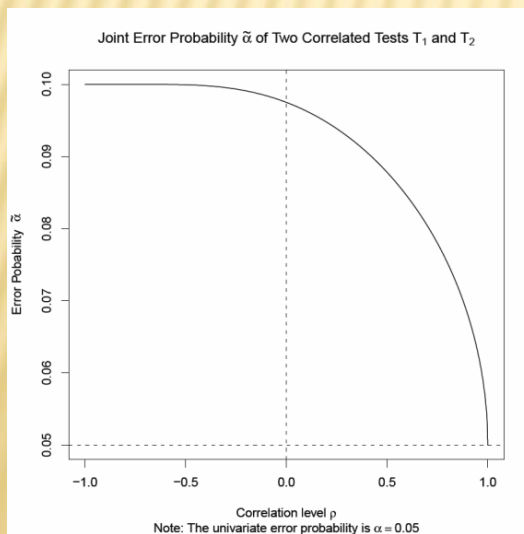
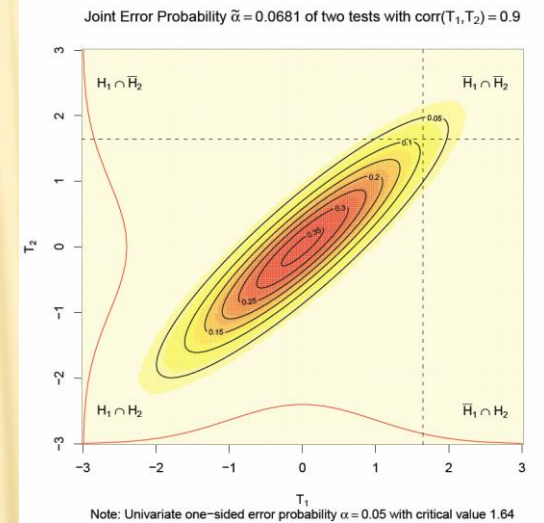
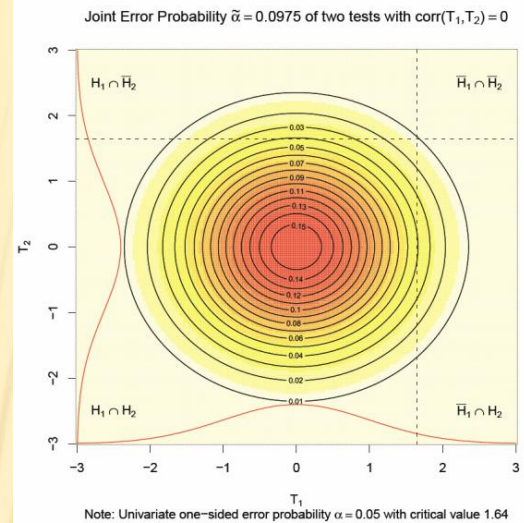
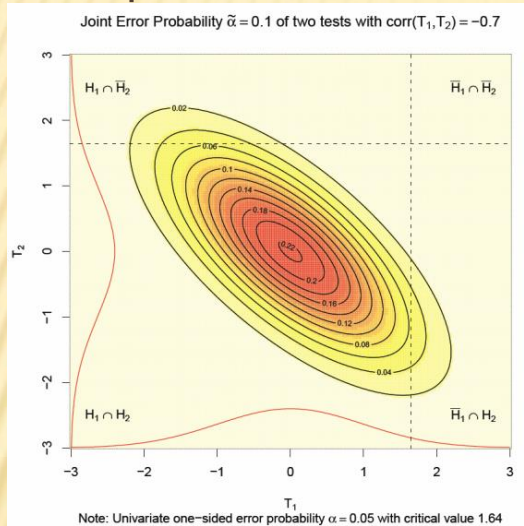
- + Feasibility study and systematic exploration of **correlation**.
- + Implementation in an open source environment.

## ✖ Future:

- + Relaxation of the underlying Gaussian assumptions
- + Efficient approximations of the **joint distribution** based on pairwise **correlation** ⇒ addressing the multiple comparison problem
- + Increased numerical performance.

# REVIEW: CORRELATION AND THE MULTIPLE COMPARISON PROBLEM

- ✗ The **correlation** among test statistics influences their joint probabilities.
- ✗ Example: Correlation among multivariate normal distributed test statistics





# REVIEW: GLOBAL AND LOCAL MORAN'S $I_i$

- ✗ Moran's  $I$  measures the degree of autocorrelation in regression residuals  $\hat{\epsilon}$ .
- ✗ Its support is bounded — but usually  $I \notin [-1, 1]$ .
- ✗ Its observed value and distribution depend on the specification of [a] the first order **spatial trend**, [b] the coded **spatial structure** and [c] the underlying **spatial process**

$$I^{obs} \leftarrow f(\mathbf{y}(\mathbf{X}, \mathbf{V}, \mathbf{\Omega})) \text{ and } F(I) \leftarrow g(\mathbf{X}, \mathbf{V}, \mathbf{\Omega})$$

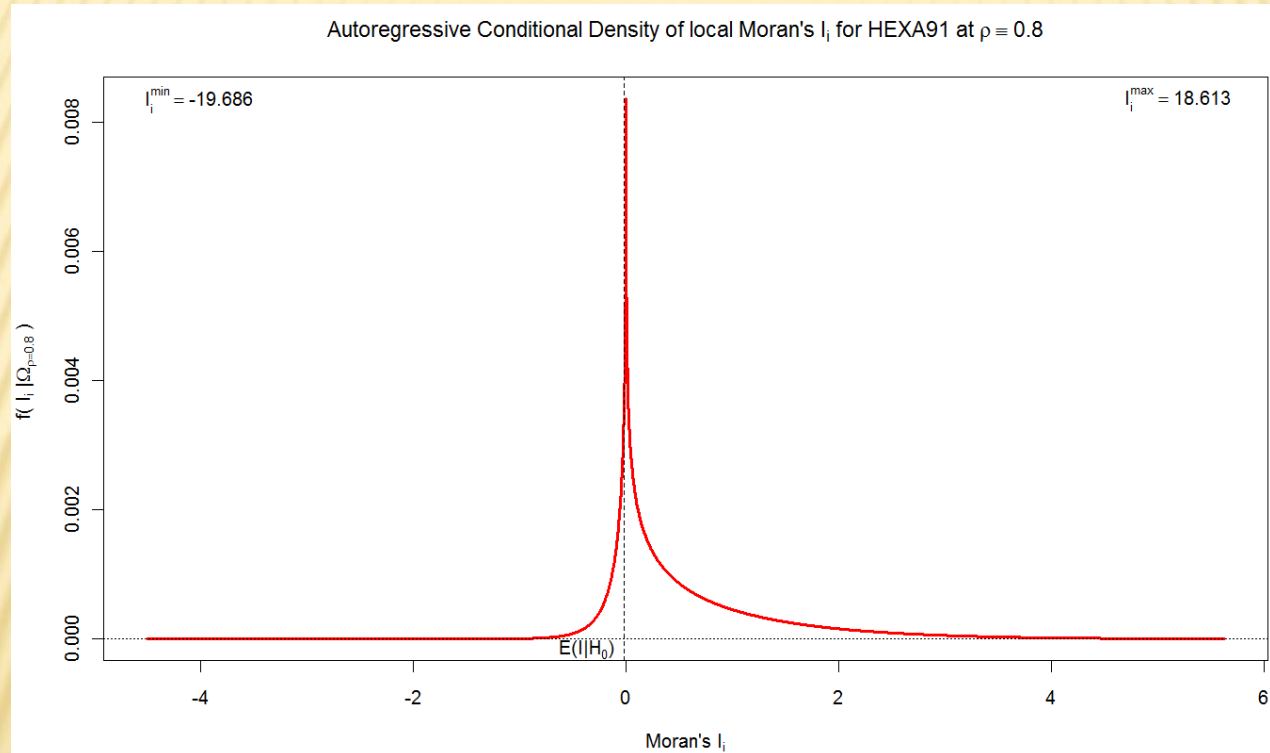
- ✗ The set of local Moran's  $I_i$ s in a map pattern relate to global Moran's  $I$

$$E(I|\mathbf{\Omega}) = \sum_{i=1}^n E(I_i|\mathbf{\Omega}) \text{ and}$$

$$Var(I|\mathbf{\Omega}) = \sum_{i=1}^n \sum_{j=1}^n \text{Cov}(I_i, I_j|\mathbf{\Omega})$$

# REVIEW: CONDITIONAL UNIVARIATE DISTRIBUTION OF LOCAL MORAN'S $I_i$

- ✗ Local Moran's  $I_i$  is not approximately normally distributed.
- ✗ Its mode is invariant of the global autocorrelation level  $\rho \in [\rho_{min}, \rho_{max}]$ .



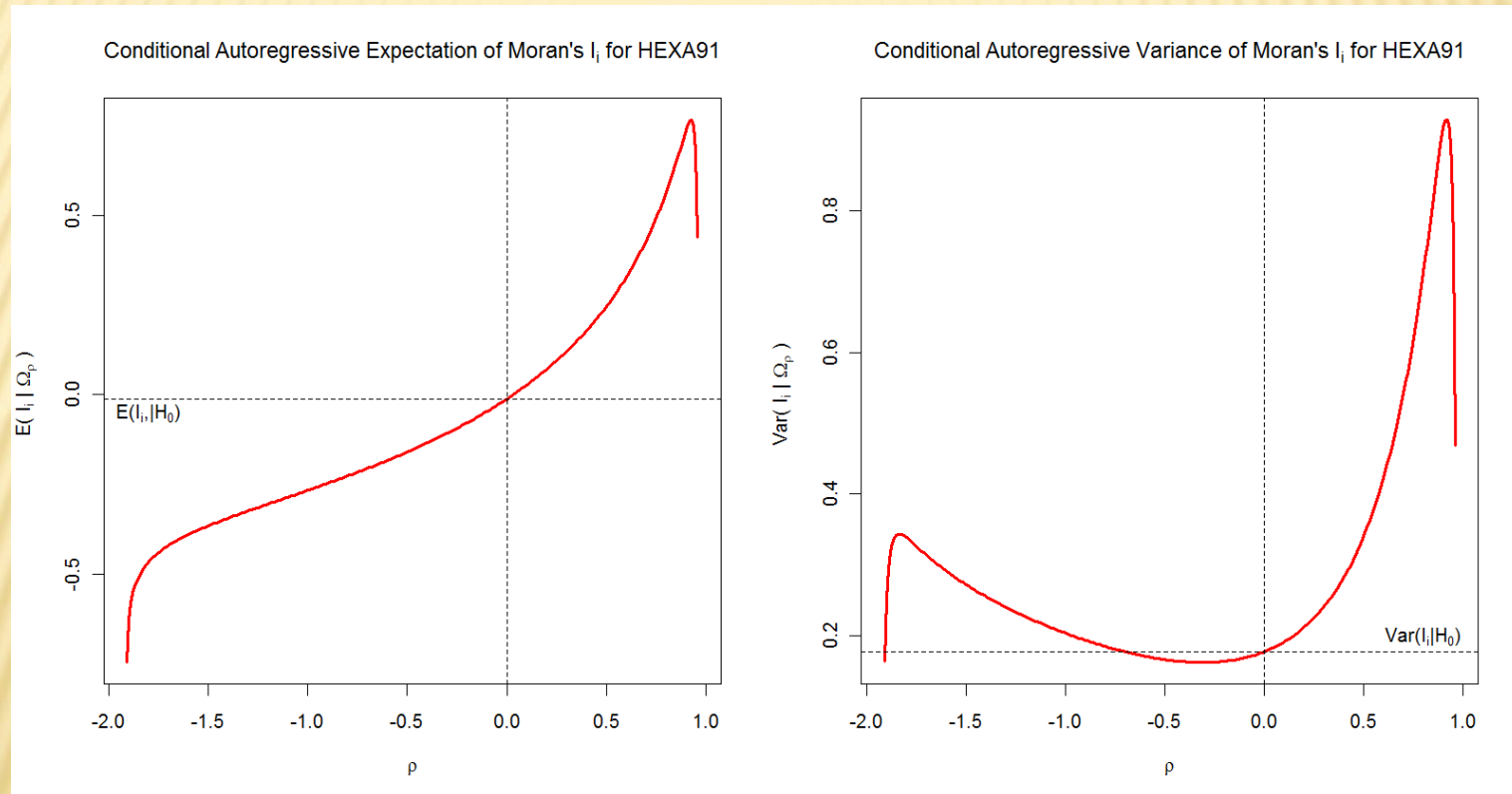
## Example:

- ✗ Interior cell with 6 neighbors
- ✗ Tessellation size  $n = 91$ .
- ✗ SAR process with  $\rho = 0.8$ .

- ✗ The probability mass shifts into the direction corresponding to the sign of the global autocorrelation level  $\rho$ .
- ✗ The feasible range and kurtosis increase with increasing tessellation size  $n$ .

# REVIEW: CONDITIONAL UNIVARIATE MOMENTS OF LOCAL MORAN'S $I_i$

- Local Moran's  $I_i$  conditional expectation and variance depend on the autocorrelation level  $\rho$  of the underlying global process.



- Notice the boundary effects at the extremes of the stationary domain of the autocorrelation levels  $\rho$ .



# REVIEW: LOCAL MORAN'S $I_i$ $p$ -VALUE DISTRIBUTION

- ✖ If a model is **properly specified** then the  $p$  -values follow  $p \sim U[0,1]$  with

$$p \equiv \Pr(I_i \leq I_i^{obs} | \mathbf{X}, \mathbf{V}, \boldsymbol{\Omega})$$

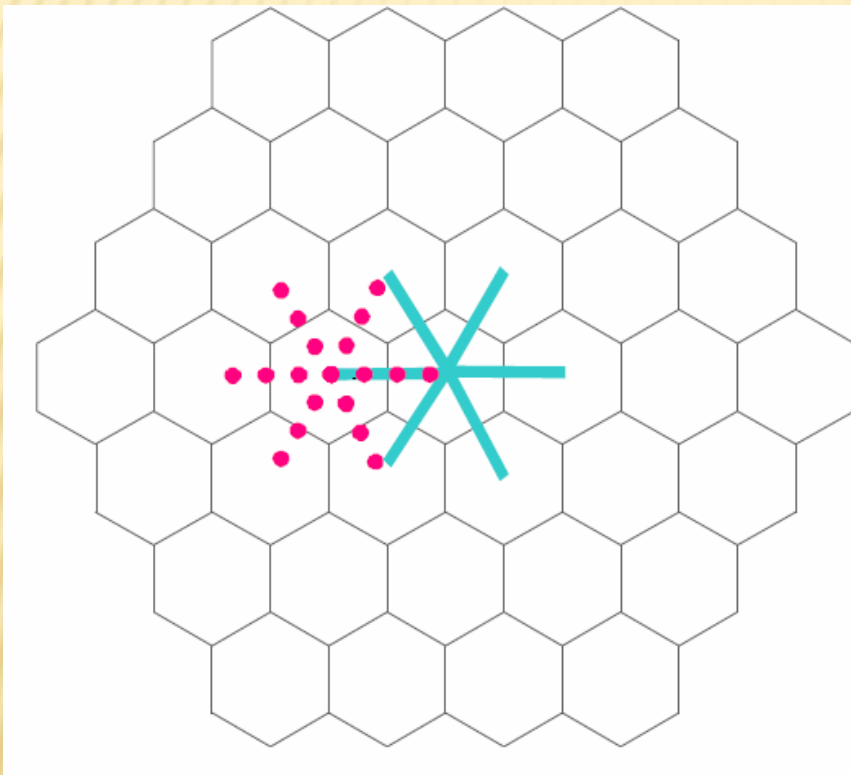
(see Murdoch et al. *The American Statistician*, 2008, pp 242-245; Rice, 2007, p 63; or Tiefelsdorf, 2000, p 136)

- ✖ Therefore, it is likely to see extreme values of local Moran's  $I_i$ s even though  $H_0$  holds true.
- ✖ The  $p$ -values of a **mis-specified** model are triangular distributed.
- ✖ This concept can be applied to an ensemble of local Moran's  $I_i$ s  $p$  -values:
  - + proper model specification implies uniform distribution
  - + the pooled  $p$  -values are **correlated**.

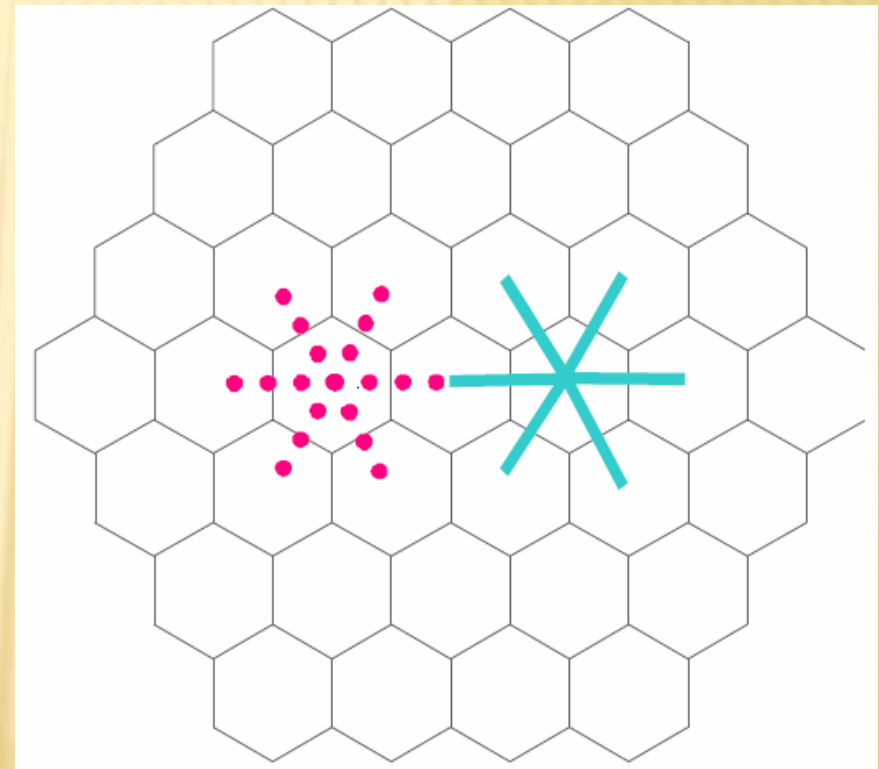


# INDUCED CORRELATION: TOPOLOGICAL RELATIONSHIPS

- ✗ The **common information** at cells, which are shared by the local structures of  $I_i$  and  $I_j$ , **induces correlation** among local Moran's  $I$ 's irrespectively of an underlying spatial process.



***Shared cells at lag 1***



***Shared cell at lag 2***

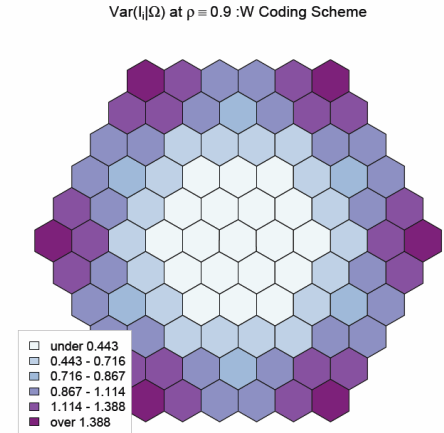
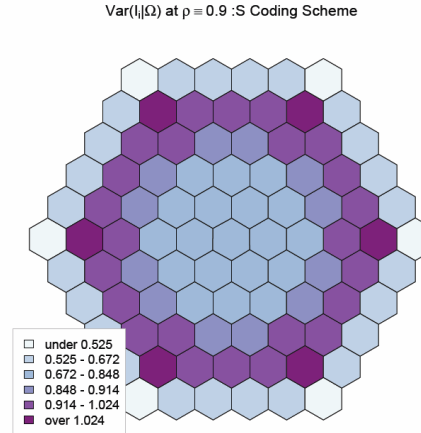
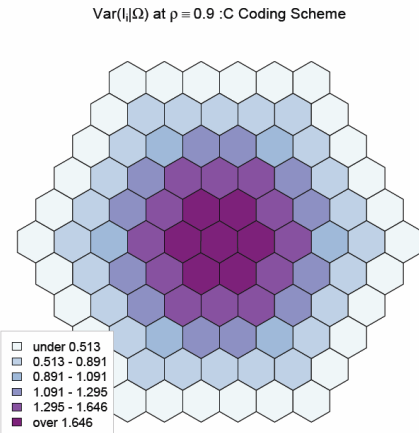
# INDUCED CORRELATION: GLOBAL PROCESSES

- ✗ **Premise:** A spatial process governs the **diffusion** or **spill-over mechanisms** of a stochastic inputs within a tessellation.  
⇒ it will have an impact on the correlation among local  $I_i$ s.
- ✗ **Process strength:** larger absolute autocorrelation levels lead to stronger signals.  
⇒ Stronger signals will tie more distant  $I_i$ s together.
- ✗ **Process specification:** **long range** SAR process versus **short range** MA process.
- ✗ **Coding Schemes:** in dependence of a cell's **connectivity** a signal at that cell is either **enhanced or dampened**.
- ✗ **Edge effects (closed system perspective):**
  - [a] on average edge cells have **lower connectivity**  
⇒ an edge signal is either enhanced or dampened depending on the coding scheme
  - [b] spill-over **signals from outside** the tessellation cannot diffuse into the closed system.

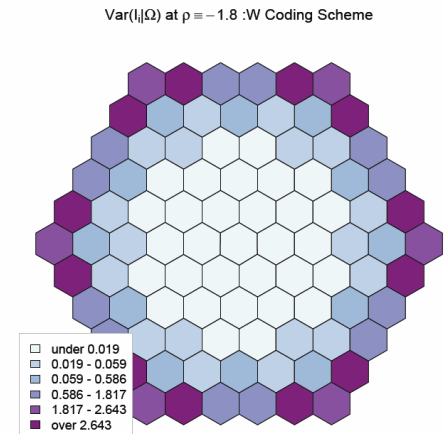
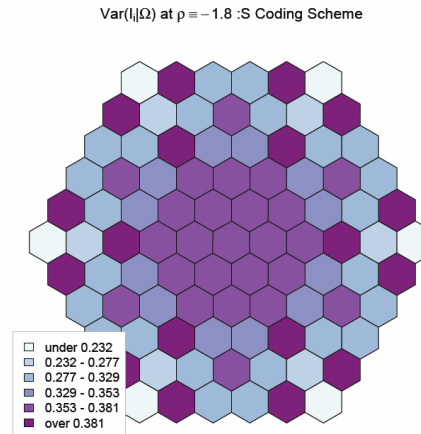
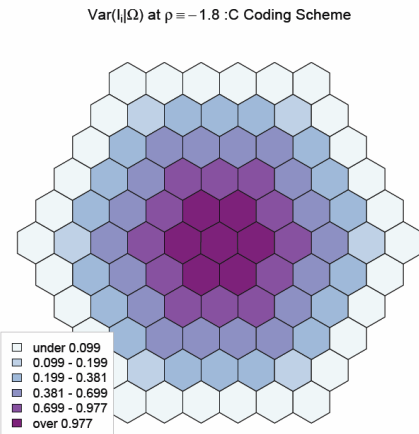
# REVIEW: LOCAL CONDITIONAL VARIANCES BY CODING SCHEME

SAR:

$\rho = 0.9$



$\rho = -1.8$



$Var(I_i|\Omega)$  is most stable in the S-coding scheme



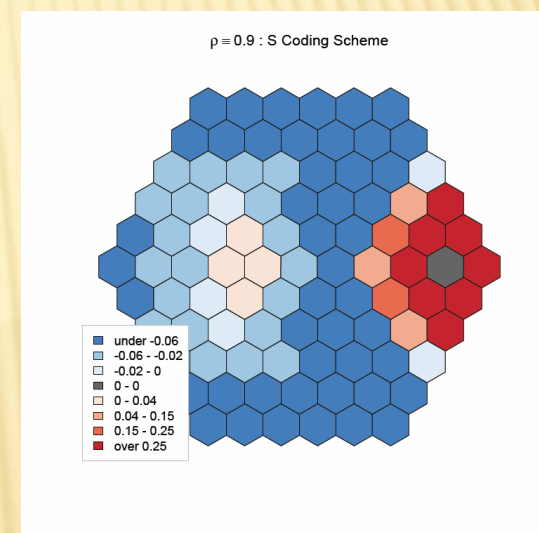
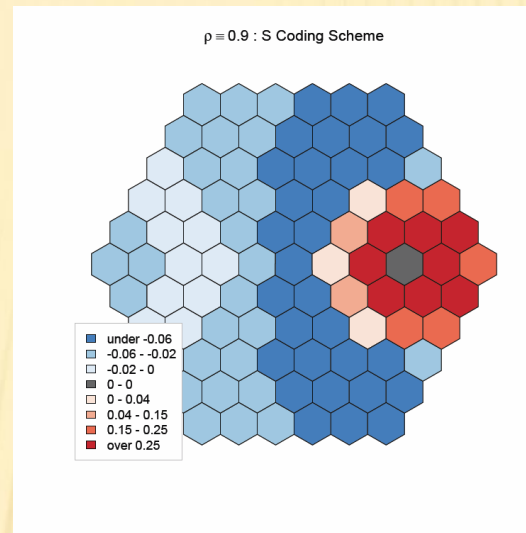
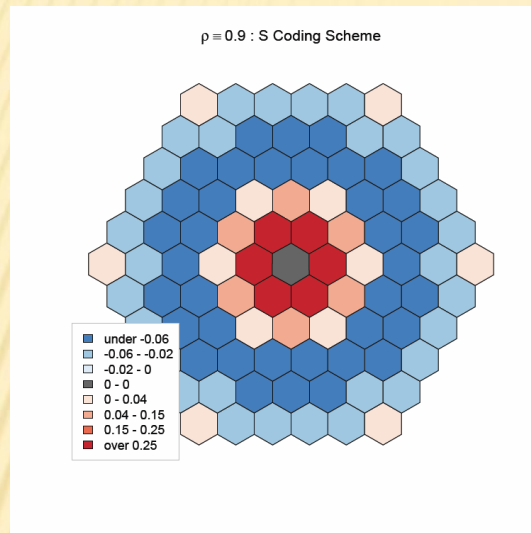
# KEY EQUATIONS TO EVALUATE $Cov(I_i, I_j | \Omega)$

- ✖ Numerical evaluation of two well-behaved **infinite** integrands using Sawa's approach to get the moments:
  - + The expectations  $E(I_i | \Omega)$  and  $E(I_i - I_j | \Omega)$ .
  - + The second moments  $E(I_i^2 | \Omega)$  and  $E([I_i - I_j]^2 | \Omega)$
  - + Both integrals depend on elaborated matrix expressions, which are not easily vectorized.
- ✖ Calculation of variances:
  - +  $Var(I_i | \Omega) = E(I_i^2 | \Omega) - E(I_i | \Omega)^2$
  - +  $Var([I_i - I_j]^2 | \Omega) = E([I_i - I_j]^2 | \Omega) - E(I_i - I_j | \Omega)^2$
- ✖ Calculation of the co-variance:
  - +  $Cov(I_i, I_j | \Omega) = \frac{1}{2} \cdot [Var(I_i | \Omega) + Var(I_j | \Omega) - Var([I_i - I_j]^2 | \Omega)]$
- ✖ In total  $n \cdot (n + 1)$  integrals need to be evaluated for all pairwise cell combinations.

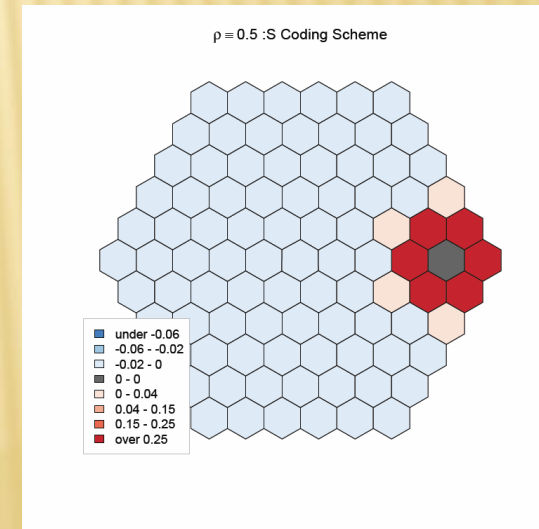
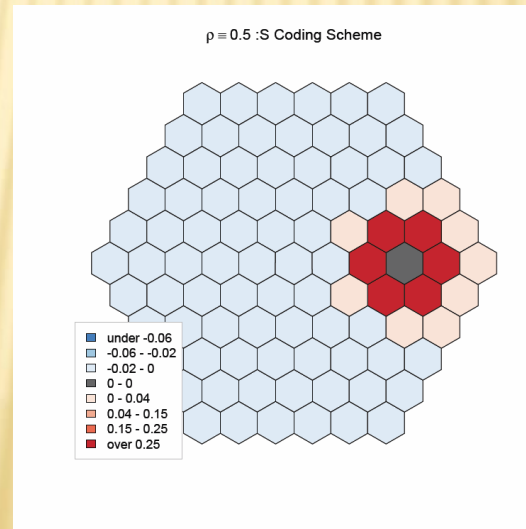
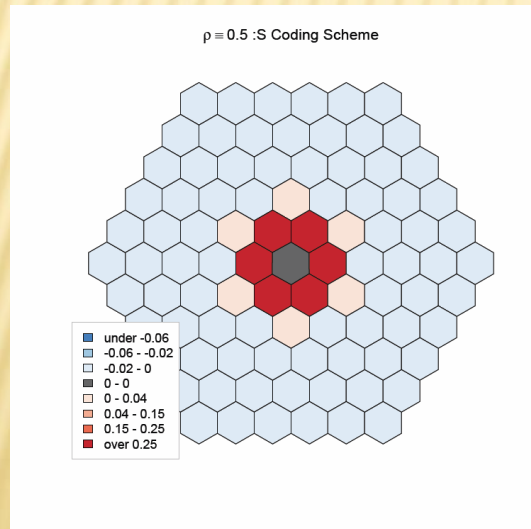
# RESULTS I: CORRELATION PATTERN BY AUTOCORRELATION LEVEL $\rho$

SAR:

$\rho = 0.9$



$\rho = 0.5$

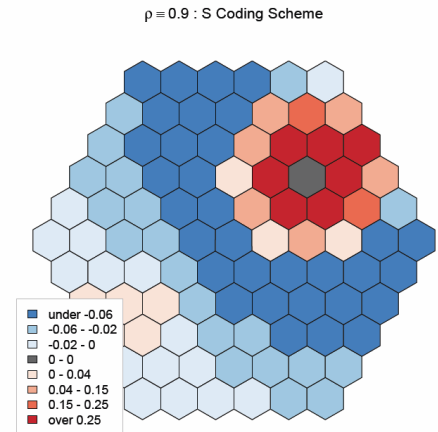
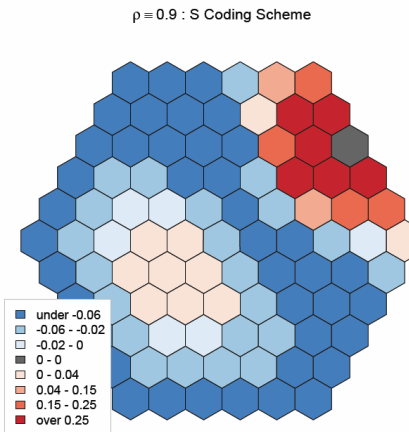
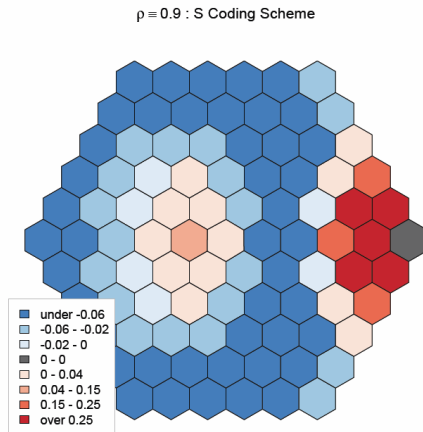


Correlation for selected reference cells in the S-coding scheme

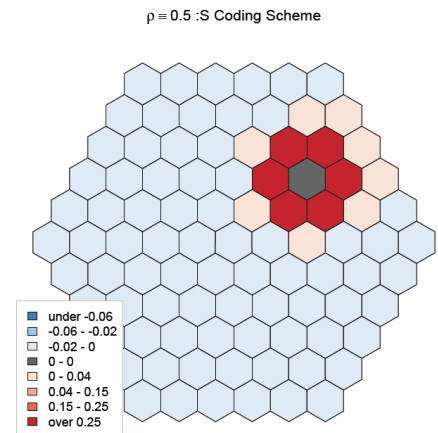
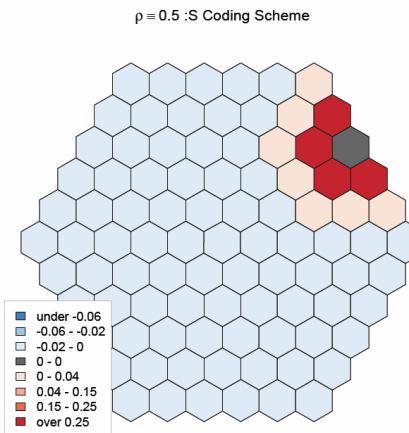
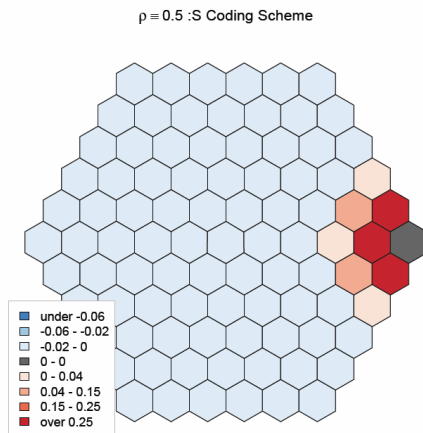
# RESULTS II: CORRELATION PATTERN BY AUTOCORRELATION LEVEL $\rho$

SAR:

$\rho = 0.9$



$\rho = 0.5$



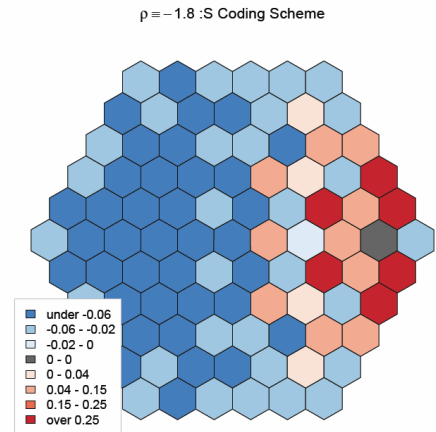
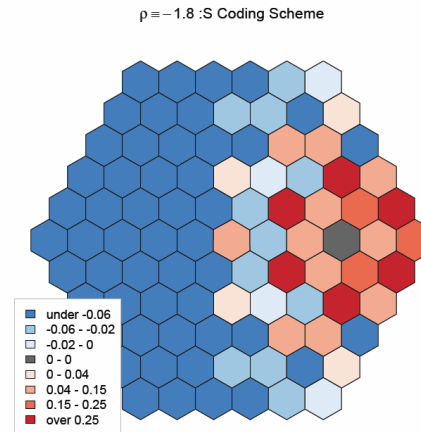
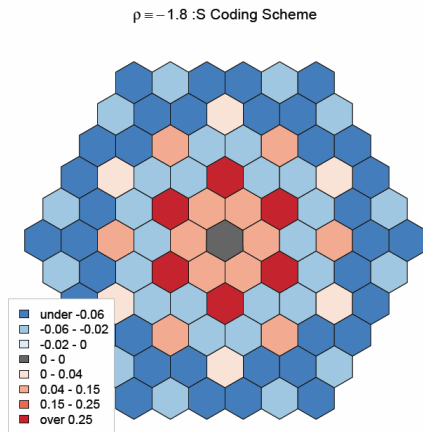
Correlation for selected reference cells in the S-coding scheme



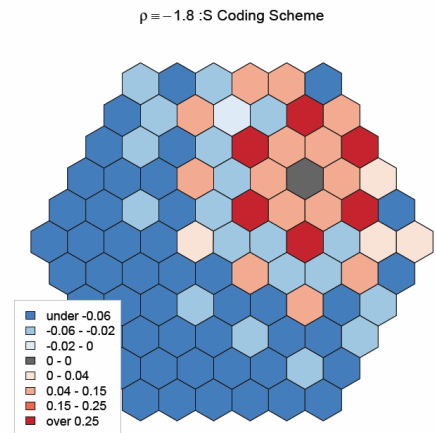
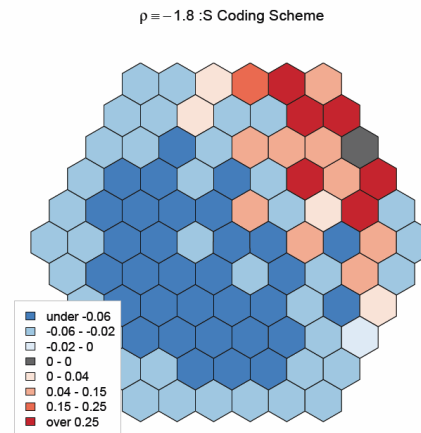
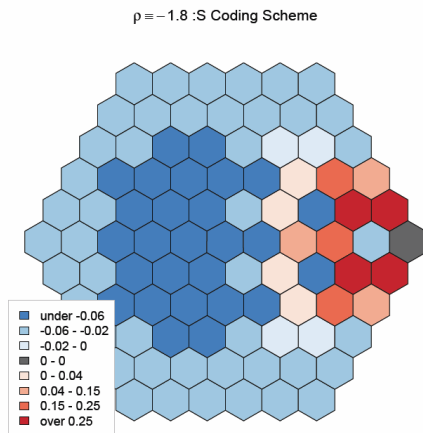
# RESULTS III: CORRELATION PATTERN BY AUTOCORRELATION LEVEL $\rho$

SAR:

$\rho = -1.8$



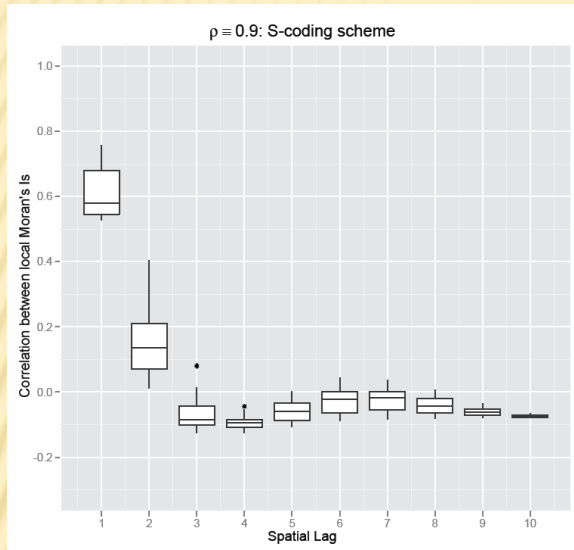
$\rho = -1.8$



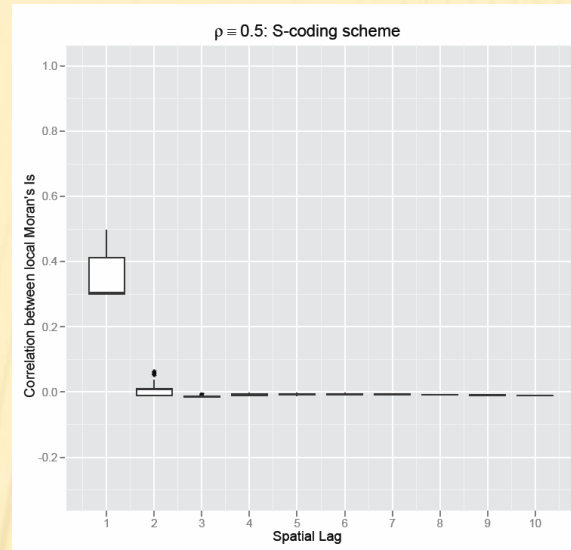
Correlation for selected reference cells in the S-coding scheme

# RESULTS IV: OVERALL STRENGTH OF CORRELATION PATTERN

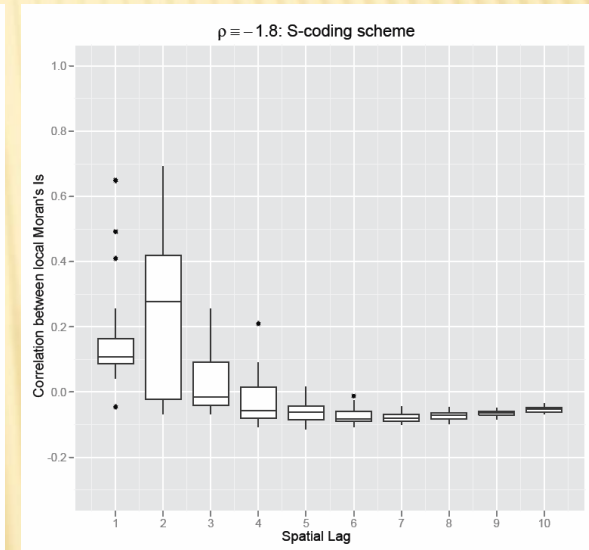
SAR:



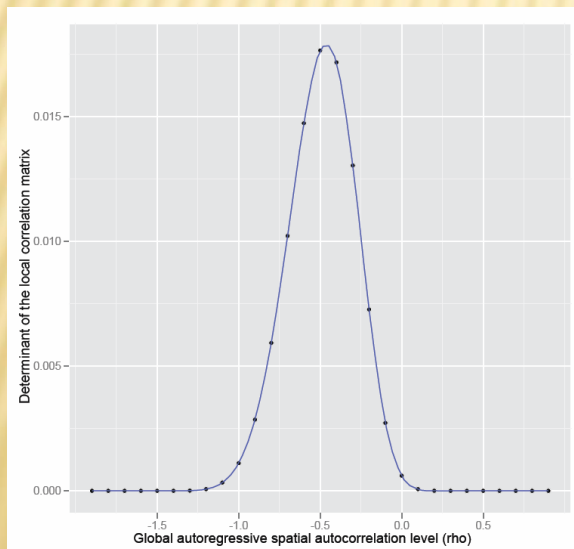
$\rho = 0.9$



$\rho = 0.5$



$\rho = -1.8$

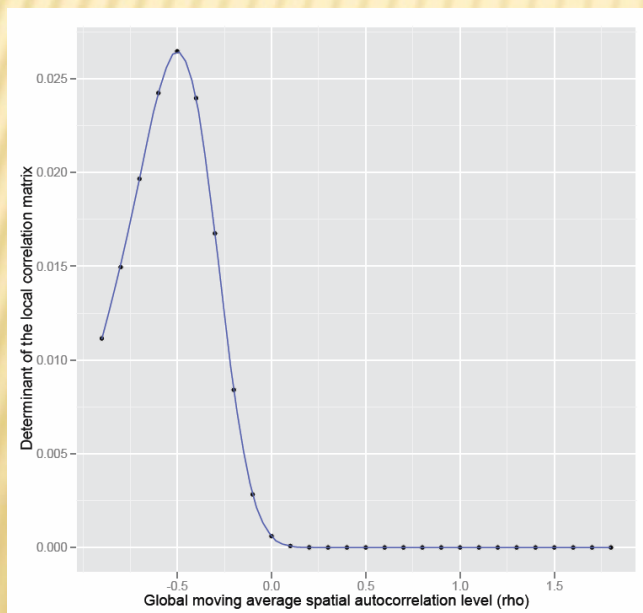
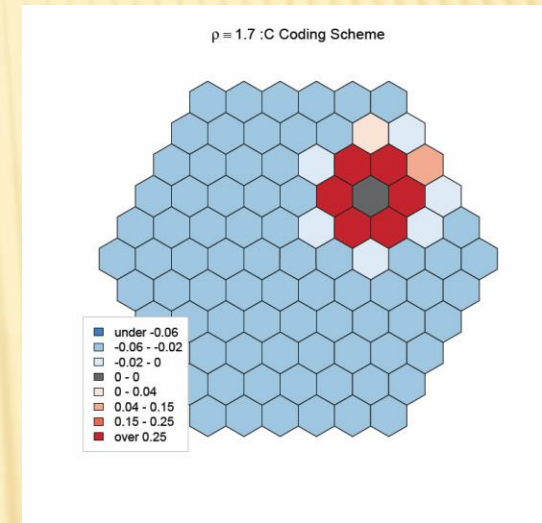
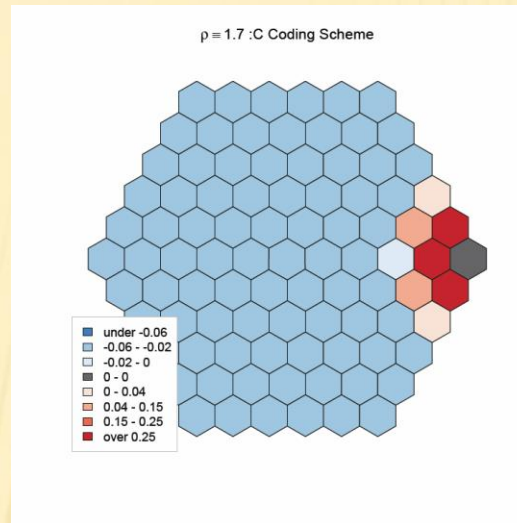
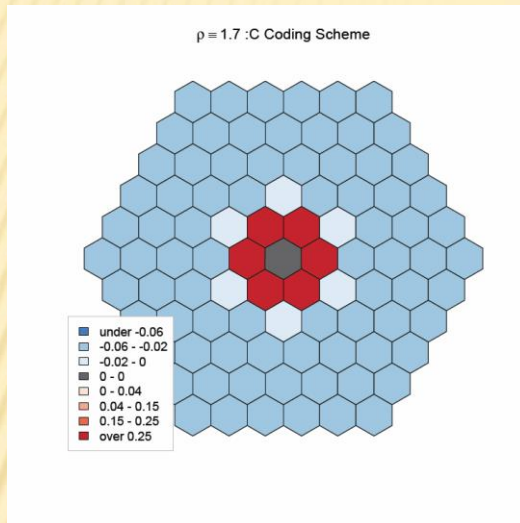


The highest degree of independence among local Moran's  $I_s$  is observed around  $\rho = -0.5$  rather than at an spatial independence level  $\rho = 0.0$ .

This holds for all coding schemes and sizes of spatial tessellations.

# RESULTS V: CORRELATION PATTERNS FOR MOVING AVERAGE PROCESSES

MA:



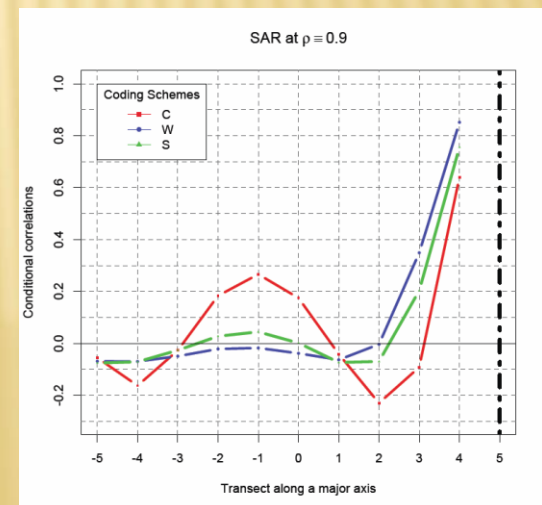
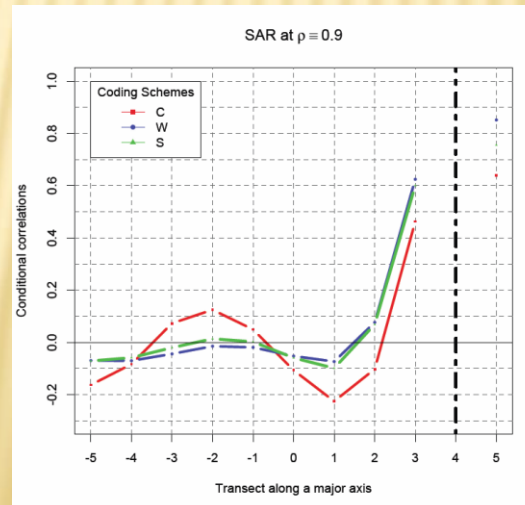
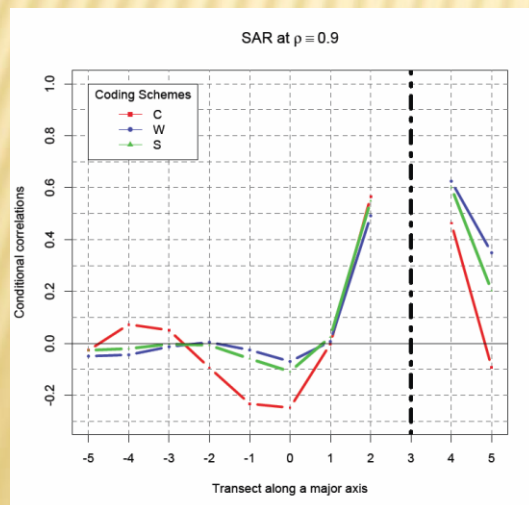
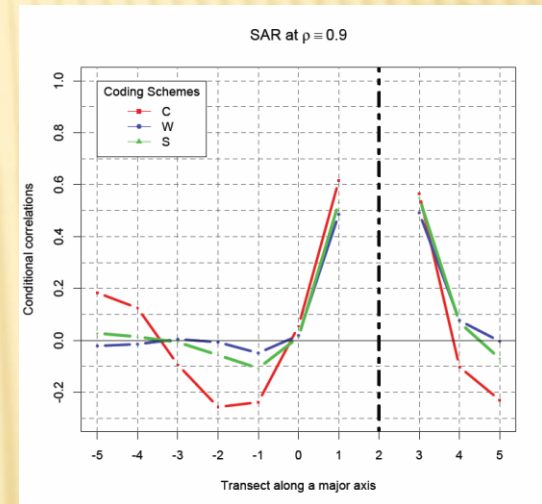
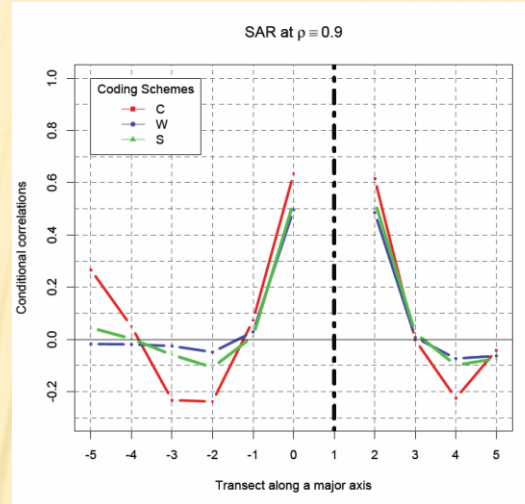
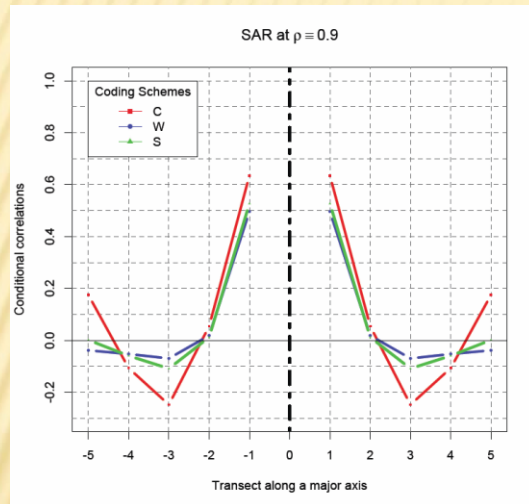
- ✗ As *theoretically expected* moving average spatial processes have a maximal topological range up to spatial lag 2.
- ✗ The degree of correlation among local Moran's  $I_i$ s depends again on the spatial autocorrelation level.



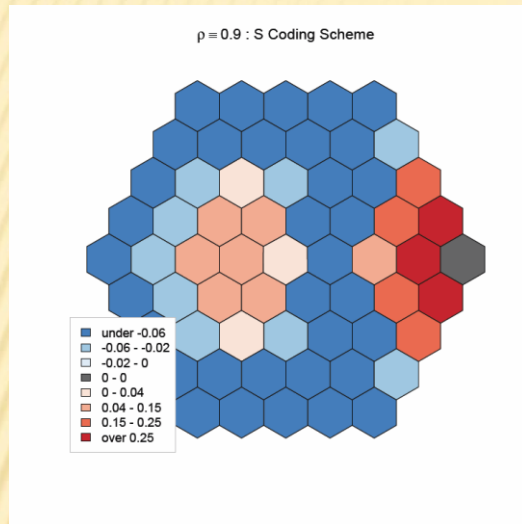
# RESULTS VI: IMPACT OF THE CODING SCHEMES ON THE CORRELATION

Correlation levels of cell pairs along a major axis transect (SAR with  $\rho = 0.9$ ).

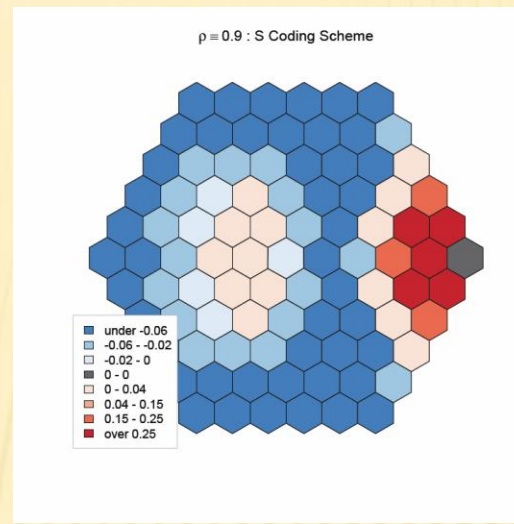
⇒ Correlation patterns of S-coding scheme is in-between the other coding schemes.



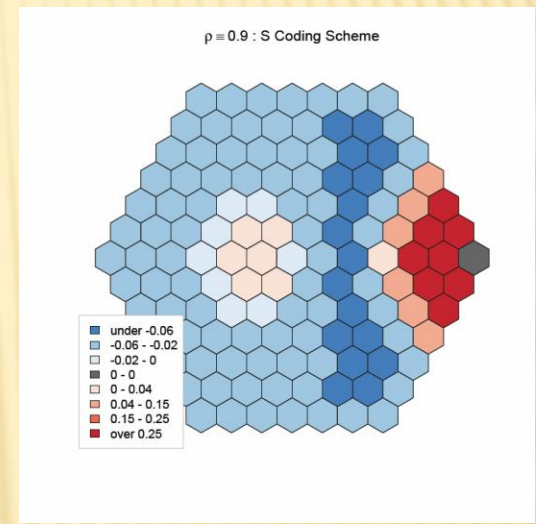
# RESULTS VII: CORRELATION PATTERNS FOR EXPANDING SPATIAL DOMAINS



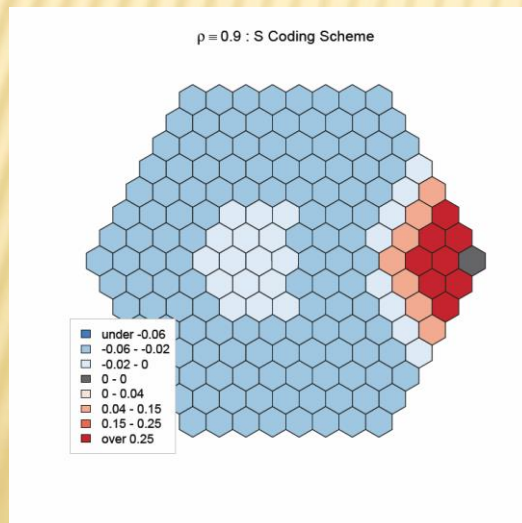
$n = 61$



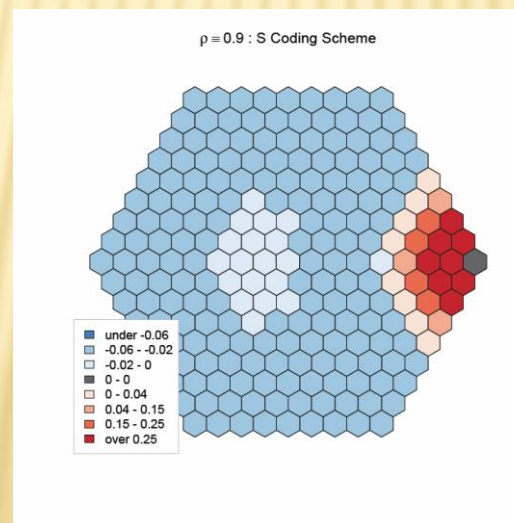
$n = 91$



$n = 127$



$n = 169$



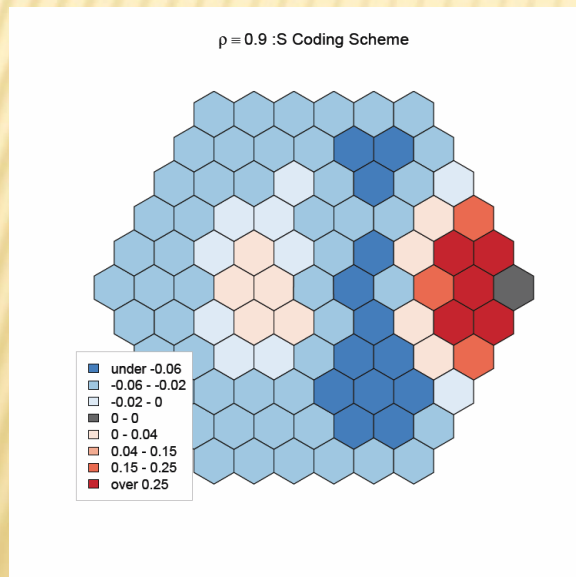
$n = 217$

- ✗ The general “echo” pattern at half the diameter due to edge reflections persists in an expanding spatial domain.
- ✗ The long-range intensity diminishes because the process exhausts its “effective” reach.

# RESULTS VIII: ACCURACY OF ANALYTICAL VERSUS SIMULATION RESULTS

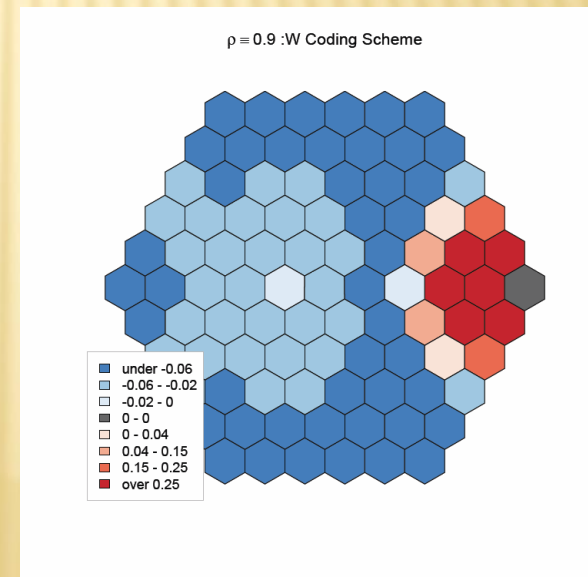
## Design of the Simulation Experiment:

- ✗ Generate 10,000 random white noise map patterns  $\epsilon \sim N(0, \sigma)$  with  $\epsilon \perp \mathbf{1}$  that satisfy the underlying assumptions of spatial independence  $z[I(\epsilon)] \sim 0$
- ✗ Transform the set of white noise inputs  $\epsilon$  into a set of autocorrelated map patterns that follow a particular spatial process specification.
- ✗ Calculated for each map pattern its associated set of local Moran's  $I_i$ s
- ✗ Evaluate at each cell the univariate distribution and for all locations the joint distribution.



Simulated Correlation Pattern

versus



Analytical Correlation Pattern




# RESULTS IX: COMPUTATIONAL EFFICIENCY

- ✗ Computational efficiency of the time consuming rejection sampling simulation approach (10,000 out of ~80,000 proposals inputs) is compared against the analytical calculations.
- ✗ A fine granular implementation with a ***parallel Basic Linear Algebra System*** (BLAS) is compared against an explicit parallel evaluation in ***independent threads*** of the correlations among local Moran's  $I_s$ .
- ✗ Results for a hexagonal tessellation with 91 cells on a 4 cores Intel I7 processor:
  - + The rejection simulation approach uses the 4 cores parallel BLAS
  - + The sequential analytical approach uses the 4 cores parallel BLAS
  - + The parallel analytical approach uses four thread and a one core BLAS
- ✗ Computational efficiency:

Rejection Simulation	Analytical Sequential	Analytical Parallel
393 sec.	222 sec.	87 sec.

# CONCLUSIONS

- ✗ With a few exceptions the conditional distribution of the Moran statistic is overlooked in the literature.
- ✗ Several open issues in spatial statistics can be addressed with the knowledge of pairwise correlations among local Moran's  $I_i$ s.
- ✗ The conditional correlation among local Moran's  $I_i$ s behaves as theoretically expected.
  - + Counter-intuitively however, the lowest degree of inter-correlations is not found at spatial independence.
- ✗ A properly specified simulation experiment is computationally more demanding and less accurate than its analytical counterpart.
- ✗ The parallel implementation of the algorithm in different  environments requires further improvements.
  - + E.g., it takes over 25 hours to calculate all 129,286 pairwise covariances of local Moran's  $I_i$ s for a model based on the 508 US State Economic Areas . However, many higher order spatial lag correlations are virtually zero and therefore can be ignored.